Egyptian Geophysical Society
EGS Journal, Vol. 20, No. 1, 67-74 (2022)

TTI VELOCITY MODEL BUILDING, TO IMPROVE SYN-RIFT IMAGING, OFFSHORE WESTERN MEDITERRANEAN, MATRUH CANYON, EGYPT

T. Elsabawy(1)*, A. El-Werr*(2) *and A. EL-Rawy*(2)

(1) PGS Company, Cairo, Egypt.

(2) Geophysics Department, Faculty of Science, Ain Shams University, Cairo, Egypt.

بناء نموذج السرعة المركب للموجات السيزميه لتحسين الصورة السيزمية للتراكيب الجيولوجية تحت الصدع الكبير، قبالة سواحل غرب البحر الأبيض المتوسط ، حوض مطروح، مصر.

الخلاصة: الارتحال الزمنى للموجات السيزميه ليس التقنية المثلى فى منطقة وادى مطروح، لانها تظهر تشوهات هندسية غير حقيقية فى شكل التراكيب الجيولوجيه ، وذلك بسبب التراكيب الجيولوجي المعقده والتغيرات الكبيره في السرعة الجانبية عبر قاعدة الوادي. من ناحية أخرى، تم اختبار الهجره العمقيه ثلاثية الأبعاد (PSDM) فى بناء نموذج سرعة ثلاثية الأبعاد، بما فى ذلك تحسين دقة نموذج السرعة بتقنية إزاحة الموجات الصغيرة. وقد تم بناء نموذج جيد كنموذج للسرعة الأولية ، يليه تطبيق سلسلة من تحديث التصوير المقطعي للانعكاس الانزلاقي في المويجات السيزميه، في وادي مطروح، غرب البحر الأبيض المتوسط، مصر .ولقد أظهرت النتائج تصويرا للتراكيب الجيولوجيه المعقدة عبر قاعدة الوادي. والفضل فى ذلك يرجع بشكل اساسى إلى نموذج السرعة عالى الدقه، الذي يمكن أن يصحح تشوهات التراكيب الجيولوجيه المزيفه فى هيكل تراكيب ما تحت الصدع، عن طريق إعادة بناء نموذج السرعه المركب لتراكيب ما تحت الصدع.

ABSTRACT: *Seismic time migration is not the optimum technique in Matruh canyon area, as it shows structurally distorted image, due to the geologic complexity and the strong lateral velocity variations across the canyon base. On the other hand, 3D Pre-Stack Depth Migration (PSDM) has been tested in which a 3D velocity model building approach, including the Beam-wavelet shift tomography. Good background velocity model was built as initial velocity model, followed by the application of series of Tilted Transversal Isotropy (TTI) wavelet shift reflection tomography update, in Matruh canyon, Offshore Western Mediterranean, Egypt. The results showed detailed imaging of the complex structural elements regime across the canyon base. This is mainly due to the high resolved velocity model, that can correct the Syn-rift structure distortions, by reconstructing the Syn-rift complex velocities.*

INTRODUCTION

The Offshore West Mediterranean, Egypt region has promising hydrocarbon potential, with the presence of proven Jurassic/Cretaceous oil and gas plays, Nile-sourced Pliocene sandstones, Bear et al.,2017, and potential pre-salt carbonate buildups analogous to the Zohr discovery. The acquired 2D and 3D seismic data helped to identify numerous deep water play types in the Matruh canyon segment (Figure 1). Most of these plays are related to the shale décollement inside the Matruh Shale Formation. Tari et al., 2012. The growth faults footwalls provide fault controlled three-way dip traps similar to the well-known rafts in the Lower Congo Basin in West Africa. Inside the rafts, the petroleum targets are located at several stratigraphic levels (plays 1 and 2). As the up-dip extension moves to the down-dip shortening, the deeper part of the area shows some imbrications. These complex toes thrust features are rapidly terminated against the Messinian salt and unconformity, defining a sub-unconformity trap (play 3). Other than these, supra-detachment play types, there might be a group of sub-detachment traps as well, and within the Jurassic syn-rift faulted blocks (play 4). Tari et al., 2012.

Imaging the subsurface of this area is a challenge, because of the poor-quality seismic data beneath the Messinian salt section and the strong lateral velocity variations across the syn-rift unconformity surface. So, the 3D PSDM including the building of a detailed velocity model, to improve the syn-rift imaging, is essential. Thus, seismic reprocessing of the available 3D acquisition vintage survey, using advanced technology and imaging techniques could help to investigate and understand well the detailed geology of the area.

The Study Area

Matruh canyon is located in the offshore part of the Egyptian coast region, that extends from the coastline, across the narrow shelf, into the relatively deep water (Figure 2). The canyon is Jurassic to Early Cretaceous rift basin. A prominent Cretaceous Shale accumulation developed within the basin to fill the Matruh Canyon, producing several listric-faults bounded supra- association hydrocarbon targets. The stratigraphy of the offshore/onshore Matruh basin is currently based only on the extrapolation of the onshore well data sets from the Western Desert (Tari et. al, 2012).

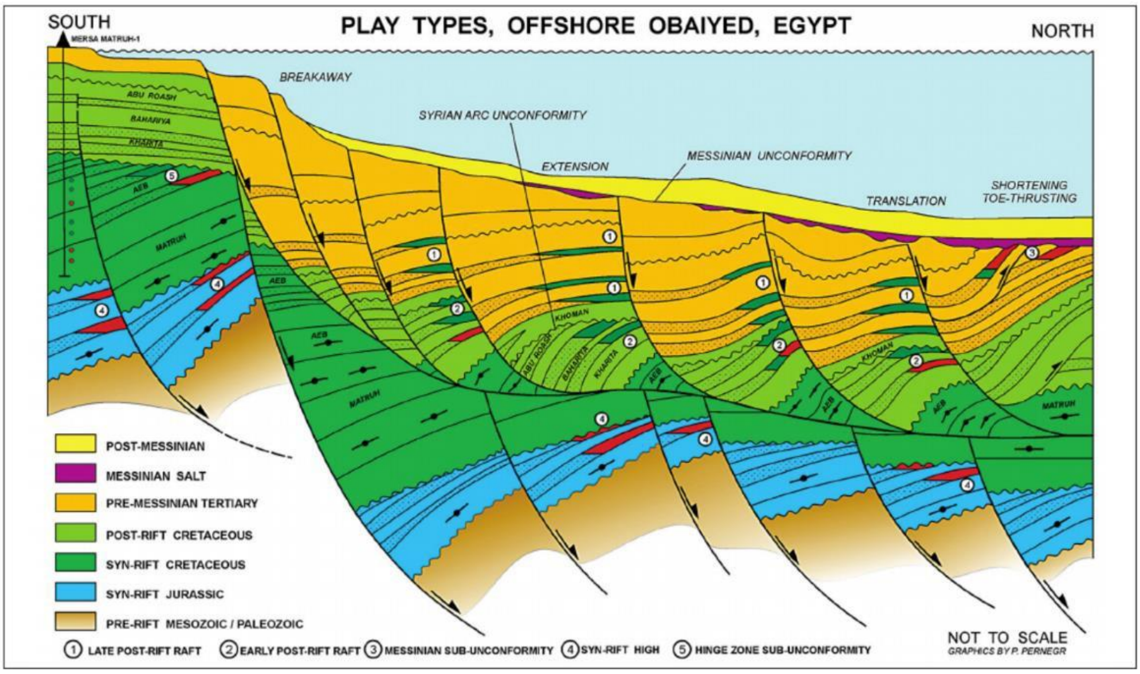

Figure (1): Offshore Matruh canyon area deep water plays types (After Tari et al., 2012).

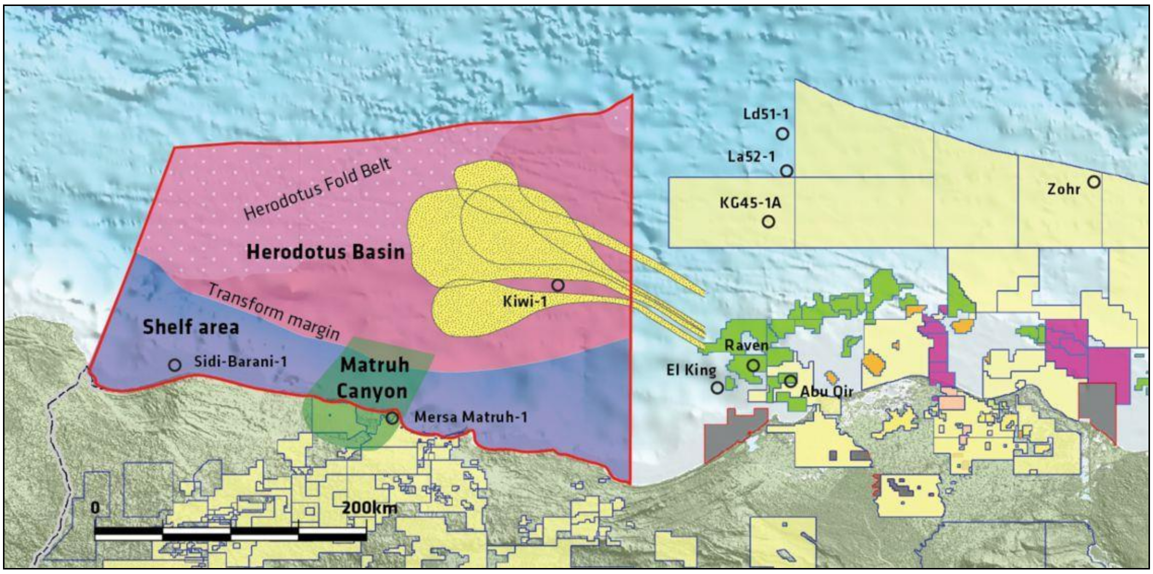

Figure (2): Location map of the Matruh Canyon study area.

The study area was covered by the PGS Multi-Client seismic data, including 3D streamer data which was acquired in 2007 with Narrow Azimuth (NAZ) acquisition geometry. The early 'time processing' at that time did not show a good image for the complex geology present.

Geologic Setting of the Study Area

To understand the tectonic elements of the shelf area, in the absence of drilled wells, the onshore Western Desert tectonics are reviewed (Figure 3). This region has undergone many phases of extension, uplifting, erosion and subsidence, resulting in locally thickened stratigraphy of Paleozoic to date. In the onshore, the most rift phase is mid-Jurassic, with normal faulting and unconformities formed by erosion of uplifted footwalls. This is often related to the initiation of continental rifting during the Triassic-Jurassic breakup of Pangea (and the opening of the Neo- Tethys Ocean). Jurassic half grabens were inverted during the onset of Tethys ocean collision (African-Eurasian plate convergence) during the Cenomanian. This compressive phase could be regionally extensive. Extension of the continental crust is generally considered to span the Lower Triassic-lower Aptian section (Tari et al., 2012, Liu et al., 2014 and Tassy et al., 2015).

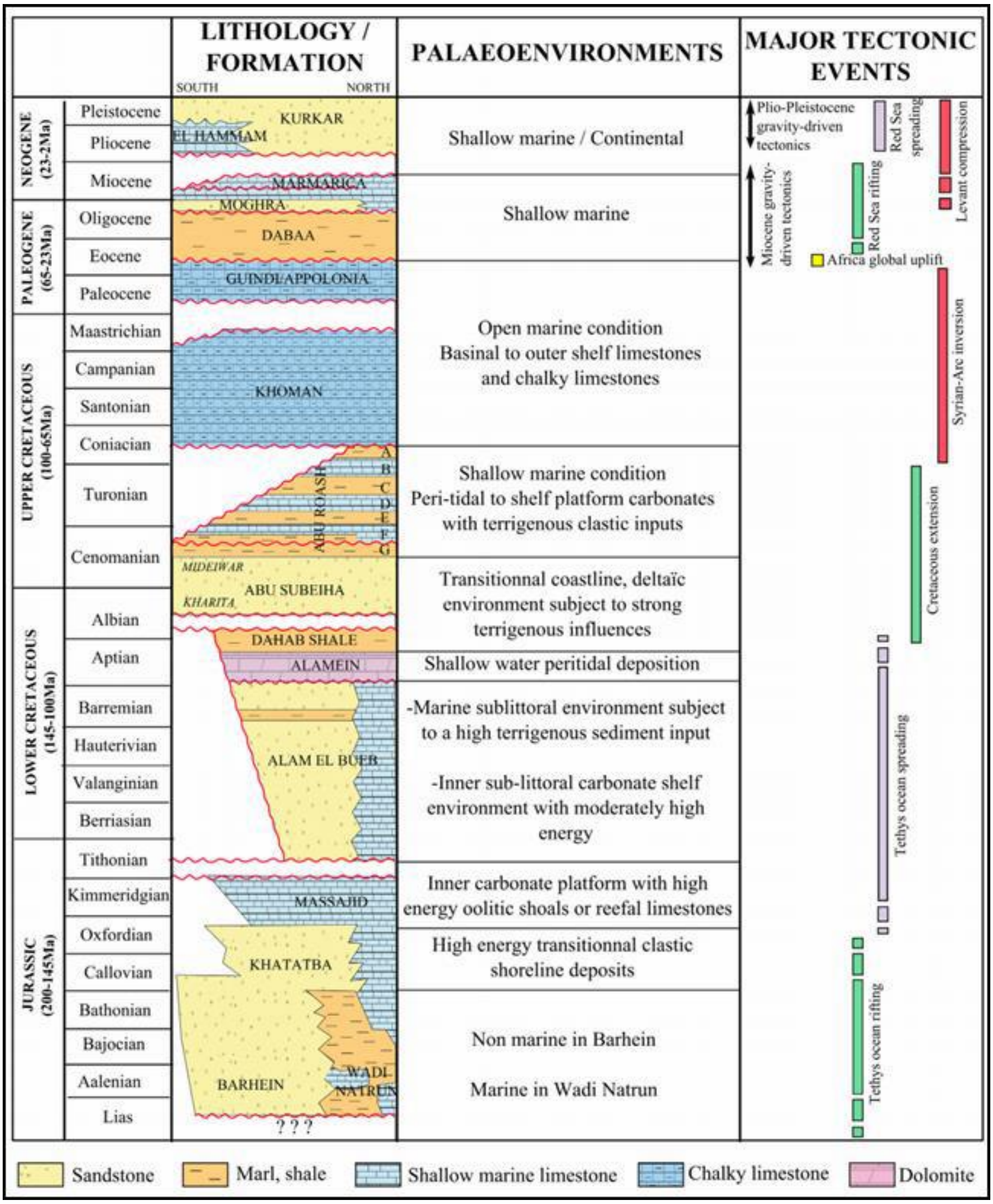

Figure (3): Regional onshore tectono-stratigraphic chart of the margin from the Western Desert to the Nile Delta. After (Tassy et al, 2015).

In the offshore, a complex geologic setting, characterized by different interactive plate boundaries, created major tectonic structures (Figure 4) and controlled the Eastern Mediterranean region. The continuous relatively changes in the tectonic regime through the geologic periods have formed this rather rugged corner of the Mediterranean Sea in a monumental way. The tectonic evolution of the Eastern Mediterranean is impacted profoundly by major geodynamic processes of the Neo-Tethys opening in the Early Mesozoic period, linked to the rifting phase from Triassic to Jurassic times. the continuous convergence of the African and Eurasian plates, since Late Cretaceous, led to the emplacement of the ophiolite bodies within the region and the expulsion of the Anatolian microplate towards the west.

The stratigraphy of the onshore/offshore Matruh canyon is based only on the extrapolation of the onshore Western Desert well data sets. Jurassic different carbonate and silicic-clastic formations are well interpreted in terms of rifting episodes, which proceeded into the Neocomian/Barremian sequence. A conspicuous unconformity on Alam El Bueib Top Formation is considered, as the extreme breakup unconformity.

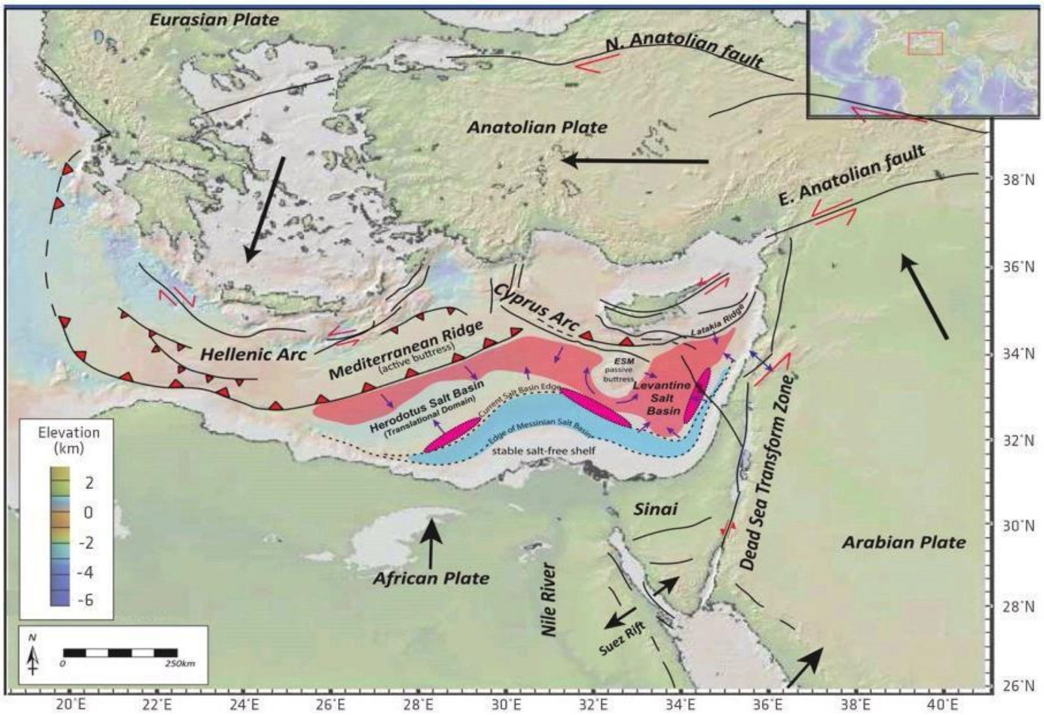

Figure (4): Eastern Mediterranean structural elements map, showing the major tectonics, after Robertson and Mountrakis, (2006 and Gardosh et al., 2008).

The famous marker of Alamein dolomite is the transgressive phase which came above the breakup unconformity. The Kharita and Bahariya clastic Formations, overlain by the carbonates and shales of Abu Roash Formation, characterized the early post-rift period. During the Santonian, reactivation of the syn-rift normal faulting happened, as the manifestation of the regional scale compressional deformation of the Syrian Arc system (Bosworth et al., 1999). The related unconformity separates the Abu Roash Formation from the overlying Khoman Formation. Localized uplifting and shortening associated with the Syrian Arc inversion continued irregularly vertically and laterally into the Paleogene.

METHODOLOGY

Kirchhoff depth migration was selected, as it is a robust and economical algorithm, to image large and complex surveys. In order to work properly, a smooth velocity model is required. It is challenging to ray-trace accurately through complex velocity models presenting sharp velocity contrasts, as the ray-tracings will behave erratically. Kirchhoff migration suffers from the additional limitation in areas of poor reflectivity, where the migration noises contaminate the weaker primary signal. To resolve those issues, an approach, using high-definition velocity update, combined with a sophisticated imaging technique was necessary to improve the seismic image.

After the completion of the time processing, the pre-processed dataset was used, to run an implementation of Beam Pre-Stack Depth Migration (BPSDM) (Sherwood et al., 2009), allowing calculation of the 3D RMO attributes for reflection tomography updates ‘PGS hyper Tomo’. Velocity model building methodologies include the two major divisions of the post-rift section, that includes (Post-Messinian, Messinian, Pre-Messinian Tertiary and Upper Cretaceous) and the syn-rift section, that includes (Lower Cretaceous, Jurassic and Mesozoic).

Velocity Model Building Experience in East Mediterranean

The earth-velocity model-building approach in marine environment starts with the water velocity layer. Usually, a scan of constant velocities is performed, to check the variation of velocity at different water depths. The optimum velocity, that flattens the common image gathers (CIG) in depth at the water bottom (WB), will be noted against the depth to the WB. The velocity function V(Z) = (Vo + k Z) is generated, where Vo is the starting velocity, Z is the depth of the WB and k is the vertical gradient, that determines the change in velocity. Some surveys include temperature- salinity (T-S) curves measured at different locations across the study area. The T-S curves are utilized, whenever the salinity of the water changes (i.e., offshore Nile Delta environment) or the temperature significantly changes from shallow to deep water. In most cases T-S curve-derived function can be better used.

For the post-Messinian section, earlier model-building techniques used a simple starting velocity (Vo) and gradient (k) from well data. If the sonic well information is sparse or not evenly distributed over the area, then a smoothed Dix interval velocity model (Dix, 1955) is inverted from a pre-stack time migration RMS velocity and used as an initial velocity model. In locations with known anisotropic parameters, an initial anisotropic model is built, using area-specific Thomsen delta (δ) and epsilon (ε) values. If the anisotropic parameters are not confirmed from well information or the area includes variable compaction regimes, not covered by well information, then the initial model is built for isotropic medium, followed by several isotropic tomography updates before the anisotropy is inserted.

With a few wavelet-shift vertical transverse isotropic (VTI) or tilted transverse isotropic (TTI) grid tomography passes (Sherwood et al., 2011) are performed over the initial model, the final post-Messinian section can be well imaged in depth. In the presence of Pliocene gas sand channels, special interpretation for those channel bodies is required to separate the sand channels from the rest of the background velocity model. A variable Q-inverted model can be embedded to compensate the signal attenuation and dispersion.

Also, a simple starting velocity and a vertical gradient can best fit the pre-Messinian section down to the carbonate platform across both the Levant and Herodotus basins, while in Matruh canyon, the early post-rift raft deposits required different velocity regimes. In regions where the salt thin out to form local salt/anhydrite pockets, the starting model is analogous to the pre- Messinian section and will be followed by a series of focused tomography updates (El-Bassiony et al., 2016 and Battisttuti et al., 2018). This is the most complicated region to image the Messinian and the pre-Messinian sections. The Messinian thick salt layer velocity changes from 4200 m/s in Herodotus basin to 4300 m/s in the Levant Basin. The pre-Messinian flood velocity starts from 2400 m/s and gradually increases with a gradient of k = 0.2 s-1 and clipped velocity to 3500 m/s, where the detrital Miocene section is present.

Building Velocity Model in Matruh Canyon.

The water layer velocity is built, using an average function of the measured temperature- salinity (TS) curves. Below the water layer, the model was divided into two major units (post-rift and syn-rift), where the Messinian evaporites thin out. The post-rift unit thickness is very thin towards the shoreline and very thick in the deep-water bottom. Building the post-rift section in Matruh canyon is challenged by the absence of well information. The Dix interval velocity inverted from the pre-stack time migration velocity is smoothed spatially and used as an initial velocity model. After a few global tomography updates, the anisotropic parameters delta (δ) and epsilon (ε) (Thomsen, 1986) along with the Slope-X and Slope-Y are also introduced to perform the Tilted Transverse Isotropic (TTI) depth migration and tomography updates to position the complex structures more accurately. A zero Thomsen's delta value was given for the whole model, due to the absence of well information, while the epsilon (ε) value was scanned. The scans determined a good gradient model from 200 m below the WB at epsilon = 2 % to the canyon base at 4 %.

The following steps (Figure 5) are applied, to update the velocity model, using the reflection tomography. Reflection tomography nowadays is a very common and robust tool, to update the velocity models. The reflection wavelet-oriented tomography solution makes a direct use of the wavelet level properties, as determined in the Beam migration. Listed below are the steps involved:

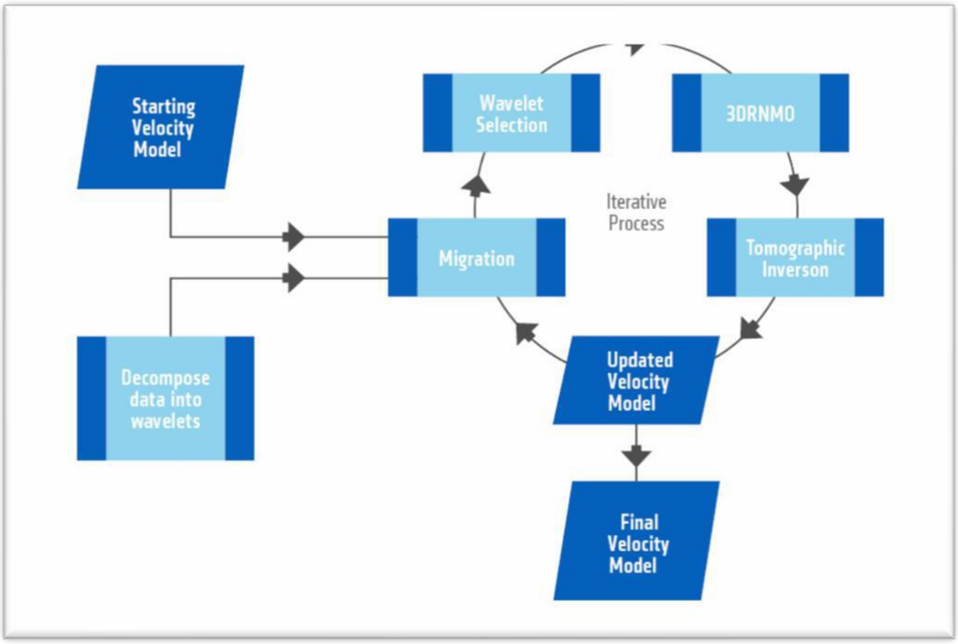

Figure (5): PGS Wavelet-shift tomogrsphy Workflow, to update the velocity model.

1) The input data are dip decomposed into wavelets.
2) In the migration step, these wavelets are mapped to the migrated location, using the current earth model. A reconstruction workflow, then allows these wavelets to be reconstructed in the migrated space.
3) 3D Residual Normal Moveout determines the time shift to align the wavelets with a reference stack.
4) Finally, the velocity model is getting updated by inversion using these 3D Residual Normal Moveout (RNMO) shifts.

Layer based, the global and hybrid updating can be performed in an efficient manner. In general terms, updating is performed to increase depth and down to shorter wavelengths, as we progress through the model building. Wavelet-shift reflection tomography provides extremely high-resolution updating due to the density of the picking. To conclude with the regional velocity model building exercise, Syn-rift velocity flood was tested and applied, using 3D variable Vtop varies from 3500–5500 m/s and velocity gradient range of 0.3–0.9 s-1, where the maximum velocity clipped to 6000 m/s, followed by few passes of TTI wavelet-shift tomography velocity updates to improve the velocity resolution in the deep section (Figure 6).

TTI Kirchhoff Pre-Stack Depth Migration (KPSDM) was performed using the final achieved Depth velocity models to output migrated CDP gathers. Finally, the post migration processing was applied, to attenuate the residual noises before stacking and minor adjustments of the stacking velocity. The post-stack processing was seeking to improve the signal-to-noise ratio, by attenuating the residual random noises to improve the temporal and spatial resolution, using the application of Q-compensation (the amplitude term). A comparison between the final stacks of the legacy Kirchhoff Pre-Stack Time Migration (KPSTM) and Kirchhoff Pre-Stack Depth Migration (KPSDM) took place (Figure 7), to evaluate the imaging improvements. It can be observed from the comparison that, the Kirchhoff PSDM shows good improvements, compared to the legacy Kirchhoff PSTM, as follows:

1) Post-rift sediments are resolved and nicely image the fault planes.
2) Attenuation of the apparent structural distortion of the Matruh canyon base and syn-rift sediment blocks.
3) Syn-rift reflectors continuity.
4) Imaging the shallow carbonate platform.
5) Nicely imaged the steep-dip events.

The final depth velocity model has successfully managed, to outline the major structure and stratigraphic units in the area. The syn-rift Jurassic and Cretaceous Carbonate (Khatatba and Khoman) Formations showed up at the base of Matruh canyon. The final TTI tomography updated velocity model showed clear velocity contrast across the survey between the post-rift clastic sediments and syn-rift carbonate platform. The comparison with the legacy PSTM showed a clear image improvement.

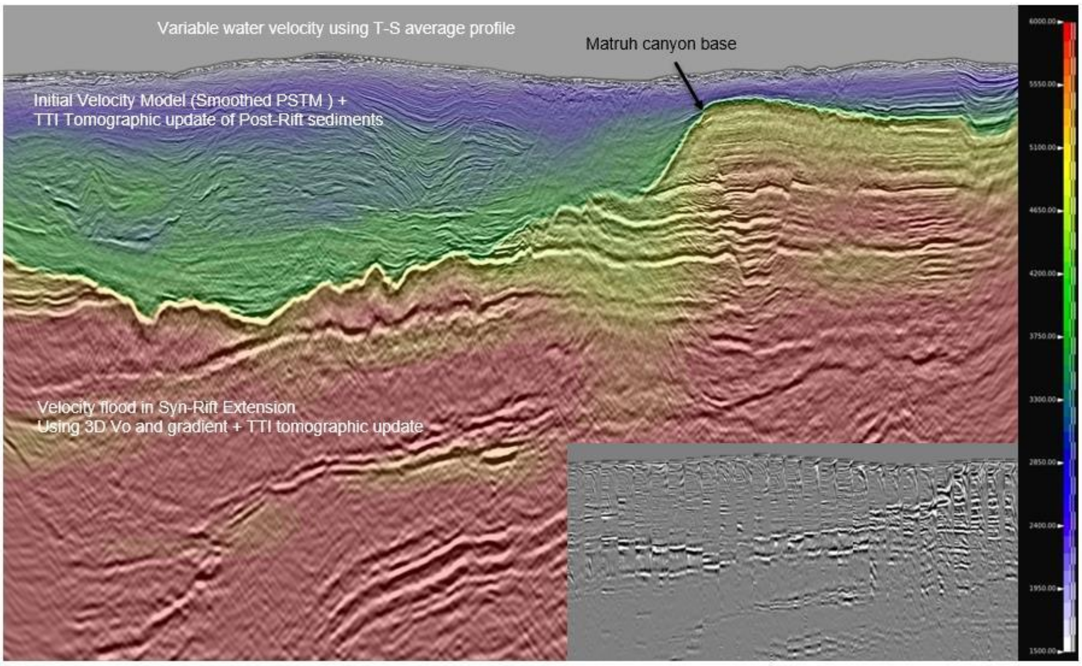

Figure (6): Matruh depth image and velocity overlay. Final vertical velocity depth model over a Kirchhoff depth image shows the post-rift and syn-rift sections in depth domain. The Beam gathers are displayed to show the gather flatness in depth domain.

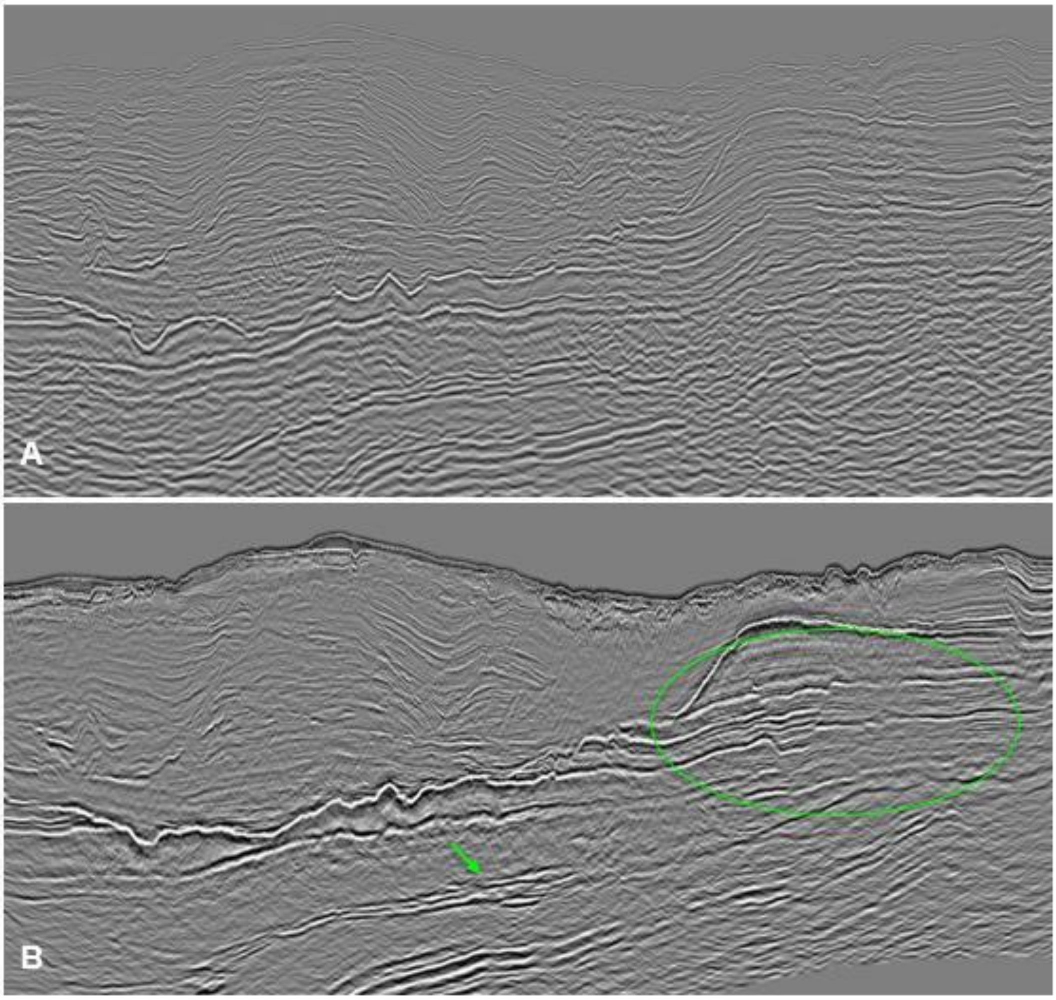

Figure (7): Comparison between the final full offset legacy Kirchhoff PSTM stack (A) and the full offset new Kirchhoff PSDM (B), the comparison is in the time domain.

CONCLUSIONS

Matruh canyon is a NNE trending Jurassic to Early Cretaceous rift basin, inverted in the Late Cretaceous-Early Tertiary. A prominent Cretaceous shale accumulation has been developed within the basin fill of the Matruh canyon, producing several listric-faults bounded supra- association hydrocarbon targets. Imaging the subsurface of this area is a challenge, because of the poor-quality seismic data beneath the Messinian salt section and the strong lateral velocity variation across the syn-rift unconformity surface. So, building a detailed velocity model to improve the syn-rift imaging is essential.

The final depth velocity model approach has successfully managed, to outline the major structural elements and stratigraphic units in the area. The syn-rift Jurassic to Cretaceous

Carbonate (Khatatba and Khoman) Formations are showed up at the base of Matruh canyon. The final TTI tomography updated velocity model showed clear velocity contrast across the survey between post-rift clastic sediments and syn-rift carbonate platform. The comparison with the legacy PSTM showed a clear image improvement. The final velocity model missing the very high frequency velocity details at the shallower part, can be driven by the application of Full Wave Inversion (FWI), that is recommended for further work.

Acknowledgements: Authors wish to thank and express appreciation to Egyptian General Petroleum Corporation (EGPC), Egyptian Natural Gas Holding Company (EGAS) and PGS MultiClient Egypt for providing the data and the authorization to publish such work. Grateful thanks are also given to the PGS Cairo imaging team for the valuable assistance.

REFERENCES

Aal, A. A., A. El Barkooky, M. Gerrits, H. Meyer, M. Schwander, and H. Zaki, 2000, Tectonic evolution of the Eastern Mediterranean Basin and its significance for hydrocarbon prospectivity in the ultradeepwater of the Nile Delta: The Leading Edge, 19, no. 10, 1086–1102, https://doi.org/10.1190/1.1438485.

Battisttuti, E., I. Mannino, and S. di-Benedetto, 2018, Improved subsurface imaging - Karawan and North Leil case history: Presented at 9th Mediterranean Offshore Conference.

Brandesberg-Dahl, S., N. Chemingui, and A. Valenciano, 2017, FWI for model updates in large- contrast media: Presented at 15th International Congress of the Brazilian Geophysical Society and EXPOGEF, 308–312.

Cavalin, D., Y. Wong, A. Bromley, M. Farouki, and K. Agbebi (PGS), 2019, Targeted vs. regional model building and imaging, A case study from offshore Sabah Malaysia : APGCE 2019, Kuala Lumpur, Malaysia | 29 – 30 October 2019, C02 Workshop (pgs.com)

Dix, C.H., 1955, Seismic velocities from surface measurements: Geophysics, 20, no. 1, 68–86, https://doi.org/10.1190/1.1438126.

EGYPTIAN NATURAL GAS HOLDING COMPANY: Website, https://www.egas.com.eg/activities/exploration

Baer, S., O. Lie, and A. Almorshedy, 2016, New Opportunities Offshore West Egypt : GEOEXPRO, Vol. 13, No. 1, https://www.geoexpro.com/articles/2016/03/new-opportunities-offshore-west- egypt

El-Bassiony, A., S. Butt, D. Cavalin, R. Ramadan, and H. Crook, 2016, Controlled sensitivity tomography for depth imaging the NAZ surveys in the Nile Delta's Messinian: Presented at 12th Middle East Geosciences Conference and Exhibition

El-Bassiony, A., J. Kumar, and T. Martin, 2018, Velocity model building in the major basins of the eastern Mediterranean Sea for imaging regional prospectivity: The Leading Edge, https://doi.org/10.1190/tle37070519.1

Gardosh, M., Y. Druckman, B. Buchbinder, and M. Rybakov, 2008, The Levant Basin offshore Israel: Stratigraphy, structure, tectonic evolution and implications for hydrocarbon exploration: Geophysical Institute of Israel Report 429.

Robertson, A.H.F., and D. Mountrakis, 2006, Tectonic development of the eastern Mediterranean region: An introduction, in A. H. F. Robertson and D. Mountrakis, eds., Tectonic development of the eastern Mediterranean region: GSL Special Publications 260, 1–9

Sherwood, J., J. Jiao, H. Tieman, K. Sherwood, C. Zhou, S. Lin, and S. Brandsberg-Dahl, 2011, Hybrid tomography based on beam migration: 81st Annual International Meeting, SEG, Expanded Abstracts, https://doi.org/10.1190/1.3628037.

Sherwood, J., Sherwood, K., Tieman, H. and Schleicher, K. , 2009, 3D Beam prestack depth migration with examples from around the world: The Leading Edge, 28(9), 1120-1127.

Tassy, A., et al., Egyptian Tethyan margin in the Mesozoic: Evolution of a mixed carbonate-siliciclastic shelfedge (from Western Desert to Sinai), Marine and Petroleum Geology (2015), http://dx.doi.org/10.1016/j.marpetgeo.2015.10.011

Tari, G., R. Kohazy, and K. Hannke, OMV H. Hussein, OMV EGYPT B. Novotny, OMV Azerbaijan J. Mascle, Geoscience Azur, 2012, Examples of deep-water play types in the Matruh and Herodotus basins of NW Egypt : Petroleum Geoscience 18(4):443-455, The Geological Society of London, https://www.researchgate.net/publication/273942995_Play_types_of_the_deep-water_Matruh_and_Herodotus_Basins_NW_Egypt

Thomsen, L., 1986, Weak elastic anisotropy: Geophysics, 51(10), 1954-1966.